International Journal of Mechanical and Industrial Technology ISSN 2348-7593 (Online)
Vol. 5, Issue 1, pp: (53-65), Month: April - September 2017, Available at: www.researchpublish.com

Steady State Analysis of Finite Oil Journal Bearings with Variable Viscosity Including Bearing Surface Deformation

[1]Manoj Kundu, [2] S.K Mazumder, [3]M.C Mazumdar

[1]Assistant professor, Department of Mechanical Engineering, DR. B.C Roy Engineering College, Durgapur, West Bengal, India
[2]Professor, Department of Mechanical Engineering, DR. B.C Roy Engineering College, Durgapur, West Bengal, India
[3]Professor, Department of Mechanical Engineering, NIT, Durgapur, West Bengal, India

Abstract: **This paper analyses the steady state performance characteristics of a rigid rotor mounted finite oil journal bearings considering pressure depended viscosity effect including elastic distortion on the surface of bearing liner. The theoretical analysis is intended to show how the effect of elastic distortion on the journal bearing performance for three-dimensional bearing geometries. The deformation equations for bearing surface will be solved simultaneously with hydrodynamic equations considering variable viscosity. It has been observed that load carrying capacity decreases with increase of the elasticity parameter of the bearing liner for loaded bearings and load carrying capacity increases with increase of the viscosity parameter**

Keywords: **Journal bearing, surface deformation, viscosity, attitude angle, eccentricity ratio, Reynolds equation.**

I. INTRODUCTION

Journal bearings are widely used in rotating machineries to support large loads at mean speed of rotation. Regardless of significant advancement in lubrication technology, these bearings fail due to metal to metal contact when they operate below certain minimum speed especially during starting and stopping operations. In order to save cost of replacing the bearing, these bearings are provided with flexible liner. But the deformation of liner, affects the performance characteristics of the bearing particularly at high values of eccentricity ratio.

A substantial amount of work has been reported on the steady state characteristics of rotor / bearing systems. Many investigators notably O'Donoghue et al. [9], Brighton et al. [10] and Majumder et al. [8], Jain et al.[12], Chandrawat and Sinhasan [4], Oh and Huebner [18] solved the journal bearing problem considering the effect of elastic distortion of the bearing liner. O'Donoghue et al. [9] dealt the analysis with the infinitely long bearing approximation. Brighton et al.[10] described the methods of solution for finite journal bearing considering the effect of elastic distortions. Majumder et al. [8] used the numerical methods to determine the effects of elastic distortion in the bearing liner on bearing performance. Majumder [8] had done the steady state analysis.

The steady state analysis is carried out here with the displacement equations derived from the fundamental. The displacement equations thus derived were compared with those of O'Donoghue et al. [9] for two dimensional elasticity problem with axial displacements reduced to zero. The displacement equations and form of film pressure tallied completely with Majumder et al. [8] and bearing performance analysis is done considering liner deformation through parametric study of the various variables like eccentricity ratio, slenderness ratio, Poisson ratio, liner thickness to radius ratio with variation in pressure depended viscosity .

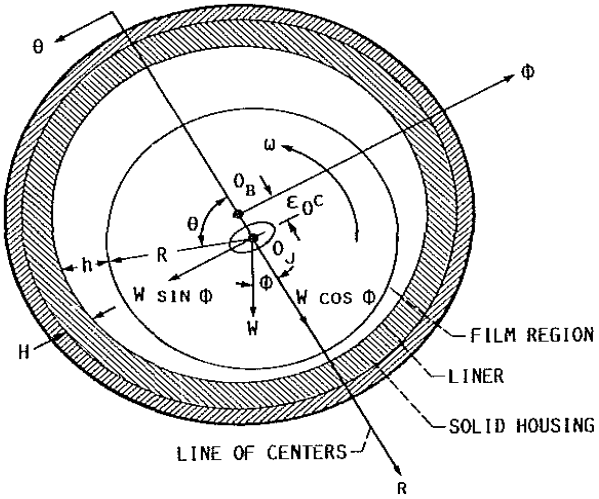

Fig. 1 shows the schematic diagram of the journal bearing with flexible liner:

II. BASIC THEORY

Using the normal assumptions in the theory of hydrodynamic lubrication, modified Reynolds equation starting from Navier-Stokes equations and continuity equation in the bearing clearance of an oil-lubricated bearing under steady state conditions may be written as

$$\frac{\partial}{\partial x}\left(\frac{h_0^3}{\eta}\frac{\partial p_0}{\partial x}\right)+\frac{\partial}{\partial z}\left(\frac{h_0^3}{\eta}\frac{\partial p_0}{\partial z}\right)=6\,\omega R\frac{\partial h_0}{\partial x} \tag{1}$$

Where h_0 is the steady state film thickness, p_0 is the steady state film pressure, η is the oil viscosity, ω is the angular velocity of journal and R is the journal radius.

The arrangement of journal bearing system with bearing liner is shown in a schematic diagram (figure 1) above. Considering case of variable viscosity it has been observe most oils increases with pressure and the following relationship is assumed similar to Majumdar et.al. [8],

$$\eta=\eta_0 e^{\alpha p} \tag{2}$$

Where α = piezo viscosity co-efficient, η_0 Viscosity of oil at the inlet condition

Assuming modified pressure function q_0 we get

$$q_0=\frac{1}{\alpha}(1-e^{-\alpha p_0}) \tag{3}$$

By using above equation (3), equation (1) is reduced to:

$$\frac{\partial}{\partial x}\left(\frac{h_0^3}{\eta_0}\frac{\partial q_0}{\partial x}\right)+\frac{\partial}{\partial z}\left(\frac{h_0^3}{\eta_0}\frac{\partial q_0}{\partial z}\right)=6\,\omega R\frac{\partial h_0}{\partial x} \tag{4}$$

Equation (4) when non-dimensionalised with the following substitutions, we have

$$\theta=\frac{x}{R},\ \bar{h}_0=\frac{h_0}{c},\ \bar{z}=\frac{z}{L/2}\quad \bar{q}_0=\frac{q_0 c^2}{\eta_0\omega R^2}$$

The modified Reynolds equation considering variable viscosity is obtained in non-dimensional form as:

$$\frac{\partial}{\partial\theta}\left(\bar{h}_0^{\,3}\frac{\partial\bar{q}_0}{\partial\theta}\right)+\left(\frac{D}{L}\right)^2\frac{\partial}{\partial\bar{z}}\left(\bar{h}_0^{\,3}\frac{\partial\bar{q}_0}{\partial\bar{z}}\right)=6\,\frac{\partial\bar{h}_0}{\partial\theta} \tag{5}$$

Boundary conditions for equation (5) are as follows

1. The pressure at the ends of the bearing is assumed to be zero (ambient): $\bar{q}_0(\theta, \pm 1) = 0$

2. The pressure distribution is symmetrical about the mid-plane of the bearing: $\frac{\partial \bar{q}_0}{\partial \bar{z}}(\theta, 0) = 0$

3. Cavitation boundary condition is given by: $\frac{\partial \bar{q}_0}{\partial \theta}\left(\theta_2, \bar{z}\right) = 0 \ and \ \bar{q}_0\left(\theta, \bar{z}\right) = 0 \ for \ \theta \geq \theta_2$

Where θ_2 is the angular coordinate at which the film cavitates.

Now from equation (3) the p_0 can be written in terms of q_0 as $p_0 = -\frac{\ln(1-\alpha q_0)}{\alpha}$

After non-dimensionalised the relation can be given as $\bar{p}_0 = \frac{\ln\left(1 - B\bar{q}_0\right)}{B}$ (6)

Where, $B =$ viscosity Parameter is expressed as

$$B = \frac{\eta_0 \alpha \omega R^2}{c^2}$$

The steady state fluid film thickness, h_0, in the case of flexible bearing can be written as,

$$h_0 = c + e_0 \cos\theta + \delta_0 \quad (7)$$

Where δ_0 is the steady state deformation of the bearing surface and it is a function of θ and z.

After non-dimensionalised the relation can be given as $\bar{h}_0 = 1 + \varepsilon_0 \cos\theta + \bar{\delta}_0$ (8)

where $\bar{h}_0 = \frac{h_0}{c}, \varepsilon_0 = \frac{e_0}{c}$ and $\bar{\delta}_0 = \frac{\delta_0}{c}$

Before finding solution to equation (5) satisfying the appropriate boundary conditions, the elastic deformation $\bar{\delta}_0$ is obtained by a method similar to that of Majumder et al. [8] and Brighton et al. [10]. In present calculation

the three displacement components $u, v \& w$ in $r, \theta \& z$ directions are solved simultaneously satisfying the boundary conditions with an approximate method, as Brighton et al. [10], to evaluate the displacements

The pressure distribution in the bearing clearance of the rigid bearing is first calculated by solving two dimensional steady state Reynold's equation. The film pressure is then expressed in double Fourier series of the form:

$$p = \sum_{m}^{l} \sum_{n}^{l} p_{m,n} \cos\frac{2m\pi z}{L} \cos\left(n\theta + \alpha_{m,n}\right) \quad (9)$$

Where $\sum^{l}$ indicates that the first term of the series is halved.

$p_{m,n}$ and $\alpha_{m,n}$ as follows,

$$p_{m,n} = \frac{4}{\pi L}\left[\left\{\int_0^{2\pi}\int_0^{\frac{L}{2}} p\cos\frac{2m\pi z}{L}\cos n\theta \, dz \, d\theta\right\} + \left\{\int_0^{2\pi}\int_0^{\frac{L}{2}} p\cos\frac{2m\pi z}{L}\sin n\theta \, dz \, d\theta\right\}\right]^{\frac{1}{2}} \quad (10)$$

$$\alpha_{m,n} = \tan^{-1}\left[\frac{-\int_0^{2\pi}\int_0^{\frac{L}{2}} p\cos\frac{2m\pi z}{L}\sin n\theta \, dz \, d\theta}{\int_0^{2\pi}\int_0^{\frac{L}{2}} p\cos\frac{2m\pi z}{L}\cos n\theta \, dz \, d\theta}\right] \quad (11)$$

$$p_{0,0} = \frac{2}{\pi L}\int_0^{2\pi}\int_0^{\frac{L}{2}} p\, d\theta\, dz \tag{12}$$

These displacements are substituted in the stress-strain relationships using Lame's constants. The six components of stresses are then used in the equations of equilibrium to obtain the following three displacement equations,

The first term of the right-hand side of equation (9) is $\frac{1}{2}p_{0,0}$.

Using the end condition of the bearing (i,e $p=0$ at $z=L/2$) we can obtain $p_{0,0}$. This term does not contribute any deformation at $z=L/2$. Its effect for the other values of z is included in the total deformation. The boundary conditions of the inner radius are

$$\sigma_r = -p,\ \ \tau_{r\theta}=0,\ \ \tau_{rz}=0 \tag{13}$$

After non-dimensionalisation, the equation (10), (11) and (12) becomes

$$\bar{p}_{m,n} = \frac{4}{\pi L}\left[\left\{\int_0^{2\pi}\int_0^{\frac{L}{2}} \bar{p}\cos\frac{2m\pi\bar{z}}{L}\cos n\theta\, d\bar{z}\, d\theta\right\}+\left\{\int_0^{2\pi}\int_0^{\frac{L}{2}} \bar{p}\cos\frac{2m\pi\bar{z}}{L}\sin n\theta\, d\bar{z}\, d\theta\right\}\right]^{\frac{1}{2}} \tag{14}$$

$$\bar{\alpha}_{m,n} = \tan^{-1}\left[\frac{-\int_0^{2\pi}\int_0^{1}\bar{p}\cos m\pi\bar{z}\sin n\theta\, d\bar{z}\, d\theta}{\int_0^{2\pi}\int_0^{1}\bar{p}\cos m\pi\bar{z}\cos n\theta\, d\bar{z}\, d\theta}\right] \tag{15}$$

And $\bar{p}_{0,0} = \frac{1}{\pi}\int_0^{2\pi}\int_0^{1}\bar{p}\, d\theta\, d\bar{z}$ (16)

where $\bar{p}_{m,n} = \frac{p_{m,n}c^2}{\eta_0\omega R^2}$, $\bar{p} = \frac{p\,c^2}{\eta_0\omega R^2}$, $\bar{z} = \frac{z}{L/2}$

The outer surface of the bearing is rigidly enclosed by the housing, preventing any displacement of the outer surface. The ends of the bearing are prevented from expanding axially, but are free to move circumferentially or radially.

The displacement components in r,θ and z directions are found from the pressure distribution, which has been expressed in a Fourier series. It is apparent that the displacements will also be harmonic functions.

These displacements were substituted in the stress-strain relationships using Lame's constants. The six components of stresses were then used in the equations of equilibrium to obtain the following three displacement equations.

$$C^*\frac{d^2u^*}{d\bar{y}^2}+\frac{C^*}{\bar{y}}\frac{du^*}{d\bar{y}}-\left(C^*+n^2\right)\frac{u^*}{\bar{y}^2}+\left(C^*-1\right)\frac{n}{\bar{y}}\frac{dv^*}{d\bar{y}}-\left(C^*+1\right)\frac{n}{\bar{y}^2}v^*-k^2u^*+\left(C^*-1\right)k\frac{dw^*}{d\bar{y}}=0 \tag{17}$$

$$\frac{d^2v^*}{d\bar{y}^2}+\frac{1}{\bar{y}}\frac{dv^*}{d\bar{y}}-\left(1+C^*n^2\right)\frac{v^*}{\bar{y}^2}-k^2v^*-\left(C^*-1\right)\frac{n}{\bar{y}}\frac{du^*}{d\bar{y}}-\left(C^*+1\right)\frac{n}{\bar{y}^2}u^*-nk\left(C^*-1\right)\frac{w^*}{\bar{y}}=0 \tag{18}$$

$$\frac{d^2w^*}{d\bar{y}^2}+\frac{1}{\bar{y}}\frac{dw^*}{d\bar{y}}-\frac{n^2}{\bar{y}^2}.w^*-C^*k^2w^{*/}-k\left(C^*-1\right)\frac{du^*}{d\bar{y}}-k\left(C^*-1\right)\frac{u^*}{\bar{y}}-n\left(C^*-1\right).k\frac{v^*}{\bar{y}}=0 \tag{19}$$

Where, $\lambda=\frac{E\nu}{(1+\nu)(1-2\nu)}$, $C^*=2+\frac{\lambda}{\mu}$, $k=\frac{2m\pi r_i}{L}$ & $\mu=\frac{E}{2(1+\nu)}$

The boundary conditions are, at $\bar{y}=1$,

$$C^*\frac{du^*}{d\bar{y}} = -\frac{1}{\mu}p_{m,n}-\left(C^*-2\right)\left(\frac{nv^*}{\bar{y}}+\frac{u^*}{\bar{y}}+kw^*\right) \tag{20}$$

$$\frac{dv^*}{d\bar{y}} = \frac{nu^*}{\bar{y}}+\frac{v^*}{\bar{y}} \tag{21}$$

$$\frac{d w^*}{d \bar{y}} = u^* k \tag{22}$$

and at $\bar{y} = \frac{b}{a}$, $u^* = v^* = w^* = 0$ (23)

The equations (17), (18) and (19) expressed first in finite difference form solving the displacement equations with the boundary conditions (20-23) the values of the distortion coefficient $d_{m,n}$ were obtained and expressed as,

$$d_{m,n} = \frac{\mu\, u^*}{R\, p} \tag{24}$$

The radial deformation δ of the bearing surface will be $\delta = u^*$

or, $$\delta = d_{m,n} \frac{R\, p}{\mu} r_i \cos\left(n\theta + \alpha_{m,n}\right) \cos \frac{2 m \pi z}{L}$$

Considering the bearing clearance is very small in compare to the diameter of the journal, the total radial deformation will be

$$\delta = \frac{R\, p_{0,0}\, d_{0,0}}{2\, \mu} + \sum_{m=0}^{\infty} \sum_{\substack{n=0 \\ (m,n) \neq (0,0)}}^{\infty} d_{m,n} \frac{R}{\mu} p_{m,n} \cos\left(n\theta + \alpha_{m,n}\right) \cos \frac{2 m \pi z}{L} \tag{25}$$

After non-dimensionalisation, the equation (25) becomes

$$\bar{\delta} = 2(1+\nu)\, F\left[\bar{p}_{0,0}\, d_{0.0} + \sum_{m=0}^{\infty} \sum_{\substack{n=0 \\ (m,n) \neq (0,0)}}^{\infty} \bar{p}_{m,n}\, d_{m,n} \cos\left(n\theta + \alpha_{m,n}\right) \cos m \pi \bar{z}\right] \tag{26}$$

Where, $\bar{\delta} = \frac{\delta}{c}$ and $F = \frac{\eta_0\, \omega R^3}{E\, c^3}$ and μ is replaced by $\frac{E}{2(1+\nu)}$

Knowing the distortion coefficient $d_{m,n}$ and using the expressions for $p_{m,n}$ & $\alpha_{m,n}$ from equations (14), (15) and also for $p_{0,0}$ from equation (16) the radial deformation in the inner bearing surface $\bar{\delta}$ at any point $(\theta, \bar{z})$ was computed.

III. STEADY STATE ANALYSIS:

The modified film pressure $\bar{q}_0$ was first obtained from equation (5) in finite difference form assuming a constant film shape and using Gauss-Seidel method with successive over relaxation scheme. After knowing $\bar{q}_0$ the distribution $\bar{p}_0$ can be found using equation (6) for a given value of B. The convergence criterion adopted for pressure is $\left|\left(1 - \left(\sum \bar{p}_{new} \Big/ \sum \bar{p}_{old}\right)\right) \leq 10^{-5}\right|$.

Then this pressure distribution was expressed as a double Fourier series as given by equation (9). The deformation equation (26) was then calculated for a given F using distortion coefficients from equation (24). The film thickness equation was then modified using equation (8). The process was repeated until a compatible film shape and pressure distribution was determined.

IV. BEARING CHARACTERISTICS

A. *Fluid film forces*:

At any point on the journal the film pressure is p_0 and the film force is $p_0 R d\theta d z$, where $R d\theta d z$ is any small segment at an angle θ with the line of centres. This will have components $p_0 R d\theta d z \cos\theta$ in the direction along the line of centres and $p_0 R d\theta d z \sin\theta$ in the direction normal to the line of centres. Component F_{r_0} of the steady state fluid film forces along the line of centres is given by,

$$F_{r_0} = 2\int_0^{\frac{L}{2}}\int_{\theta_1}^{\theta_2} p_0 \cos\theta (R\,d\theta)\,dz \tag{27}$$

where θ_1 and θ_2 are angular coordinates at which the fluid film commences and cavitates respectively.

Component F_{ϕ_0} of the steady state fluid film forces perpendicular the line of centres is given by

$$F_{\phi_0} = 2\int_0^{\frac{L}{2}}\int_{\theta_1}^{\theta_2} p_0 \sin\theta (R\,d\theta)\,dz \tag{28}$$

Using $\bar{p}_0 = \frac{p_0 c^2}{\eta_0\,\omega\,R^2}$, $\bar{z} = \frac{z}{L/2}$, $\bar{F}_{r_0} = \frac{F_{r_0} c^2}{\eta_0\,\omega\,R^3\,L}$, and $\bar{F}_{\phi_0} = \frac{F_{\phi_0} c^2}{\eta_0\,\omega\,R^3\,L}$, the non-dimensional form is given by,

$$\bar{F}_{r_0} = \int_0^1\int_{\theta_1}^{\theta_2} \bar{p}_0 \cos\theta\, d\theta\, d\bar{z} \tag{29}$$

$$\bar{F}_{\phi_0} = \int_0^1\int_{\theta_1}^{\theta_2} \bar{p}_0 \sin\theta\, d\theta\, d\bar{z} \tag{30}$$

B. Steady state load:

From the film forces in r and ϕ directions, neglecting the time dependent term in Reynolds equation, the resultant film force which is balanced by the load applied to the shaft can be calculated and the angle between load $\bar{W}_0$ and the line of centres (i,e attitude angle ϕ_0) are determined by

$$\bar{W}_0 = \sqrt{\left(\bar{F}_{r_0}^{\,2} + \bar{F}_{\phi_0}^{\,2}\right)} \tag{31}$$

$$\phi_0 = \tan^{-1}\left(-\frac{\bar{F}_{\phi_0}}{\bar{F}_{r_0}}\right) \tag{32}$$

where $\bar{F}_{r_0}$ and $\bar{F}_{\phi_0}$ are the dimensionless steady state hydrodynamic forces in r and ϕ directions respectively.

Since the film pressure has been obtained numerically for all the mesh points, integrations in equations (29) and (30) can be easily performed numerically by using Simpson's 1/ 3 rd. rule to get $\bar{F}_{r_0}$ and $\bar{F}_{\phi_0}$. The steady state load $(\bar{W}_0)$ and the attitude angle (ϕ_0) are then calculated by using equations (31) and (32).

C. End flow:

End flow takes place from the clearance space between the journal and the bearing at the two ends.

Flow from the clearance space is given by

$$Q = 2\int_0^{h_0}\int_{\theta_1}^{\theta_2} (w)_{z=\frac{L}{2}}\, R\,d\theta\, dy \tag{33}$$

Substituting the value of w, velocity component in z-direction we get

$$Q = 2R\int_{\theta_1}^{\theta_2}\int_0^{h_0} \frac{1}{12\eta}\left(\frac{\partial p_0}{\partial z}\right)_{z=\frac{L}{2}} y(y-h_0)\,dy\,d\theta \tag{34}$$

Performing integration with respect to y and non-dimensionalising, the equation will assume the form

$$\bar{Q} = -\frac{1}{6}\int_0^{2\pi} \bar{h}_0^{\,3}\left(\frac{\partial \bar{p}_0}{\partial \bar{z}}\right)_{\bar{z}=1} d\theta \tag{35}$$

Where, $\bar{Q} = \frac{Q}{\omega R^2 c}$

Non-dimensional end flow can thus be calculated first by finding numerically $\left(\frac{\partial \bar{p}_0}{\partial \bar{z}}\right)_{\bar{z}=1}$ and then numerical integration, once, the pressure distribution in the film region is known.

V. RESULTS AND DISCUSSION

The circumferential pressure distribution obtained from present method of solution has been plotted in figure 2 for various value of F for a particular bearing. It may be seen that the peak pressure decreases with increase in the elasticity parameter.

L/D=1.0, H/R=0.3, ε_0 = 0.85, ν =0.4

Fig. 2: Circumferential Pressures at the Centerline (Variable Viscosity)

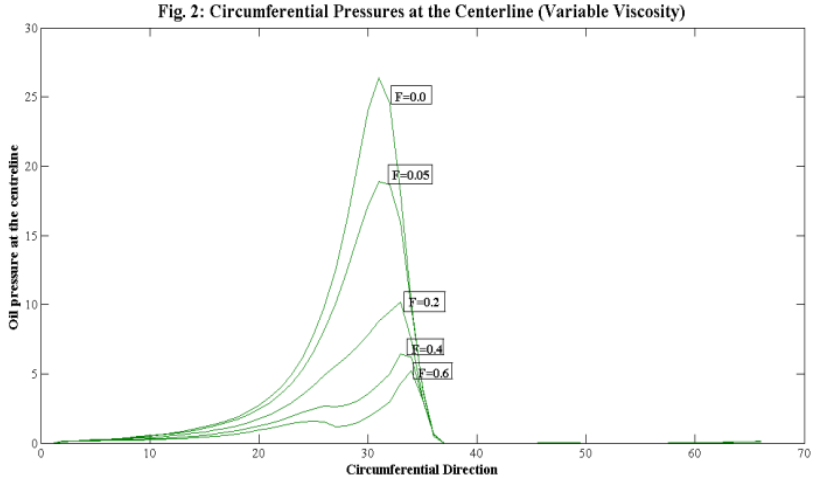

A. *Load carrying capacity*:

(a) Effect of eccentricity ratio (ε_0):

Figure.3 shows that the dimensionless load carrying capacity of journal bearings as a function of deformation factor (F) for $\frac{L}{D}=1.0,\ \frac{H}{R}=0.3,\ \nu=0.4$ when eccentricity ratio (ε_0) is considered as a parameter. From the figure it is found that when other parameters remain same as eccentricity ratio increases the dimensionless load capacity increases. Further, for the eccentricity ratio beyond 0.4 the family of the curves shows drooping trend which becomes more significant up to $F=0.4$. For the eccentricity ratio $\varepsilon_0 \le 0.4$ the characteristics are more or less horizontal meaning that the load parameter $\bar{W}_0$ remains unaffected with a change in F. The decreasing tendency of the curves at lower value of F becomes more conspicuous at higher value of eccentricity ratio (ε_0).

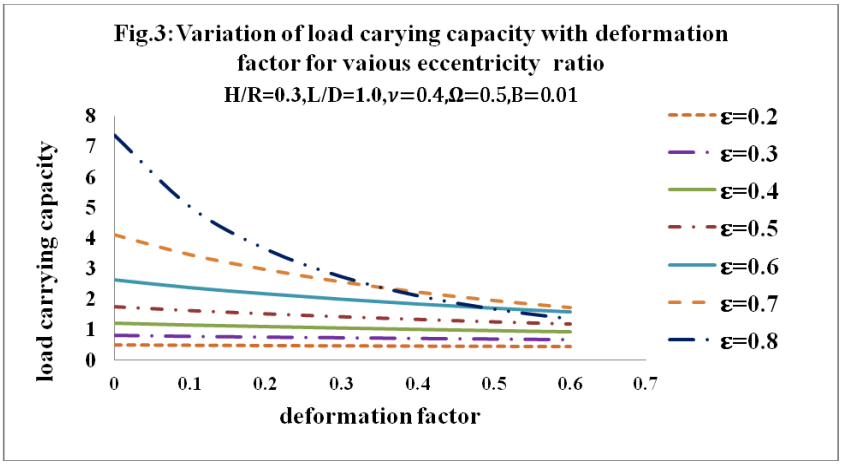

(b) Effect of slenderness ratio (L/D):

Effect of slenderness ratio L/D on the load capacity of the bearing can be studied from figure 4. Here, dimensionless load capacity of journal bearings is shown as a function of deformation factor (F) for $\varepsilon_0 = 0.6$, $\frac{H}{R} = 0.3$, $\nu = 0.4$. It is found that when other factors remain unaltered, an increase in L/D increases the load parameter. Also, the figure shows that the characteristics are more or less horizontal for $L/D \leq 0.75$ meaning thereby that for a particular L/D, the load parameter $(\bar{W}_0)$ remains unaffected by the change in deformation factor (F) at lower value of L/D.

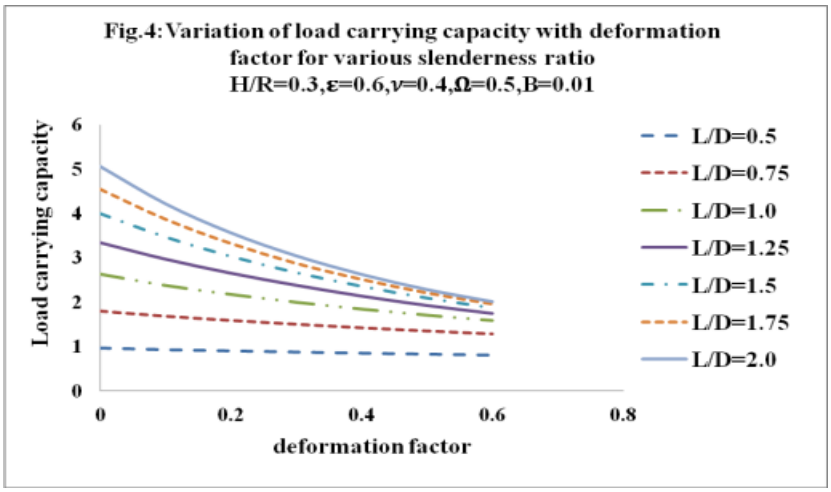

(c) Effect of Poisson's ratio (ν):

Figure.5 is the plot of dimensionless load parameter of journal bearing as a function of deformation factor (F) for $L/D = 1.0$, $H/R = 0.3$, $\varepsilon_0 = 0.6$ when Poisson's ratio (ν) is considered as a parameter. A scrutiny of the figure reveals that as Poisson's ratio increases, the dimensionless load increases. Further, the family of the curves shows declining trend i.e., the load parameter $(\bar{W}_0)$ decreases with increase in deformation factor. The decreasing trend of the curve is very slow.

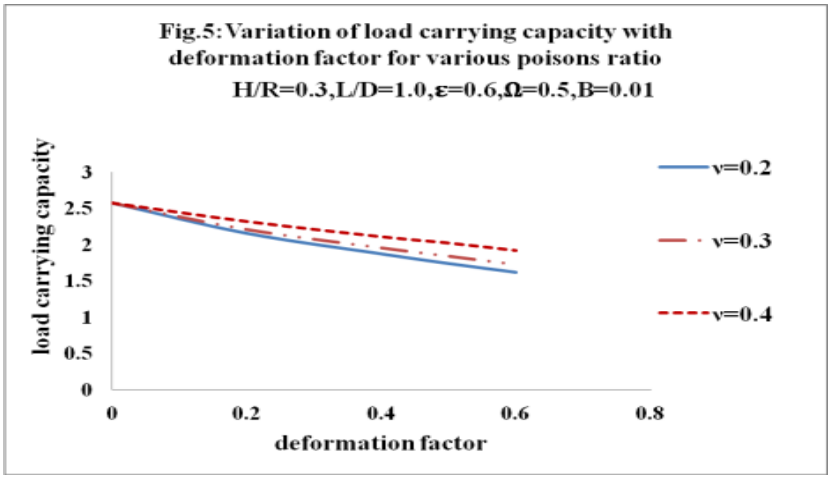

(d) Effect of liner thickness to journal radius ratio (H/R):

In figure.6 the dimensionless load capacity of journal bearings is shown as a function of deformation factor (F) for $\frac{L}{D} = 1.0, \nu = 0.4, \varepsilon_0 = 0.6$, liner thickness to journal radius ratio (H/R) is considered as a parameter. It is observed from the figure that as (H/R) increases the dimensionless load decreases. Further, the load parameter decreases initially at a slower rate and rapidly beyond the deformation factor $F = 0.3$. It is also found that the load Parameter $(\bar{W}_0)$ decreases with increase in deformation factor, when other parameters are maintained constant.

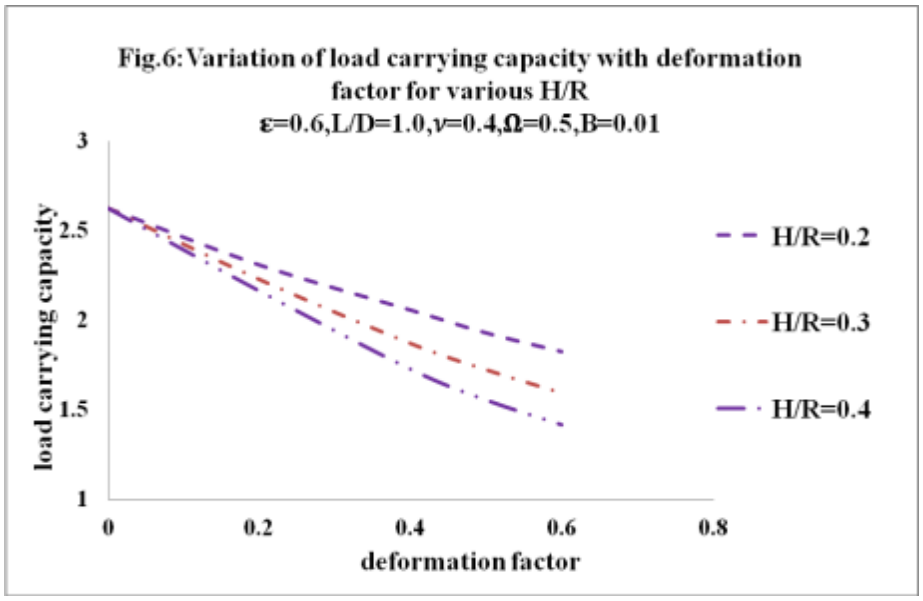

e) Figure.7 shows that the dimensionless load capacity of journal bearings as a function of eccentricity ratio (ε_0) for $\frac{L}{D}=1.0,\ \frac{H}{R}=0.3,\ \nu=0.4$ when deformation factor (F) is considered as a parameter. From the figure it is found that other parameters remain same as deformation factor increases the dimensionless load capacity decreases. Further, the dimensionless load capacity increases with eccentricity ratio. However the increasing tendency of the curves at lower value of F becomes more conspicuous at higher value of eccentricity ratio (ε_0).

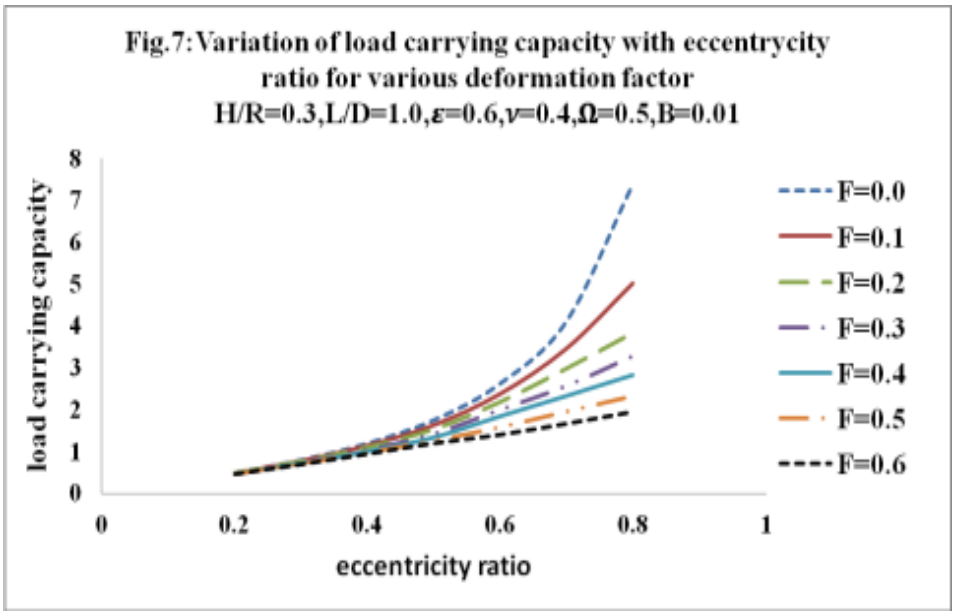

B. ***Attitude angle*:**

(a) Effect of eccentricity ratio (ε_0):

Figure.8 shows the variation of attitude angle (ϕ_0) with respect to deformation factor (F) for different values of eccentricity ratio (ε_0). It is observed from the figure that the attitude angle decreases with increase in eccentricity ratio. Further, the attitude angle increases with increase in deformation factor (F) at higher value of eccentricity ratio (ε_0). The trend of the curves, at lower value of eccentricity ratio, is more or less horizontal meaning that the attitude angle (ϕ_0) remains largely unaffected by a change in F, when all other parameters remain constant.

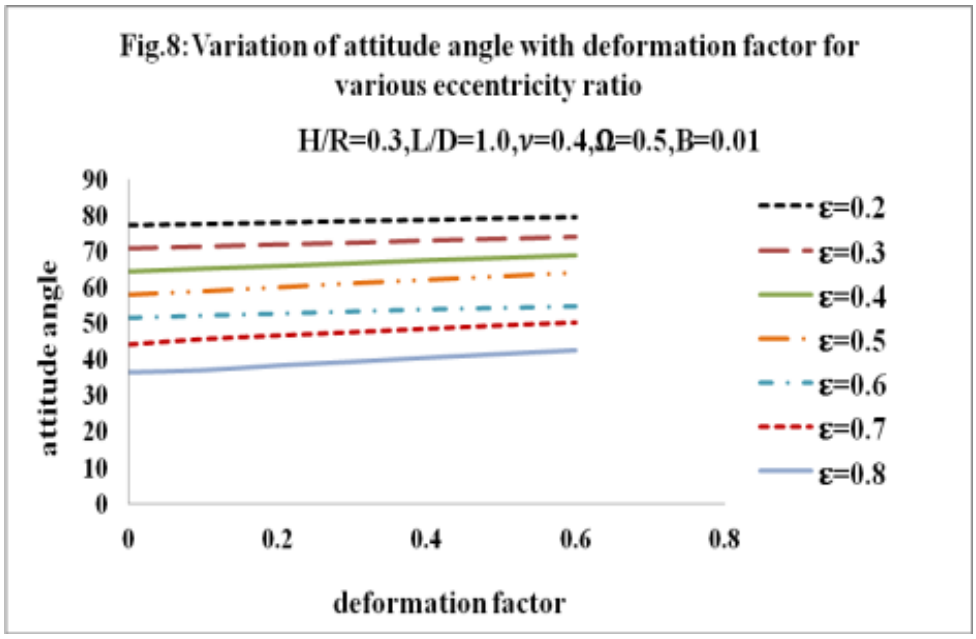

C ***End flow*:**

(a) Effect of eccentricity ratio (ε_0):

Variation of end flow (from clearance space) of the bearing with ε_0 is presented in figure.9. Non-dimensional end flow is found to increase with increase in the value of ε_0, when all other factors remain constant. It is further observed that non-dimensional end flow increases with F, and the increase is more conspicuous at higher values of ε_0 (0.8 & 0.6). At lower values of ε_0 the variation is rather small and almost negligible.

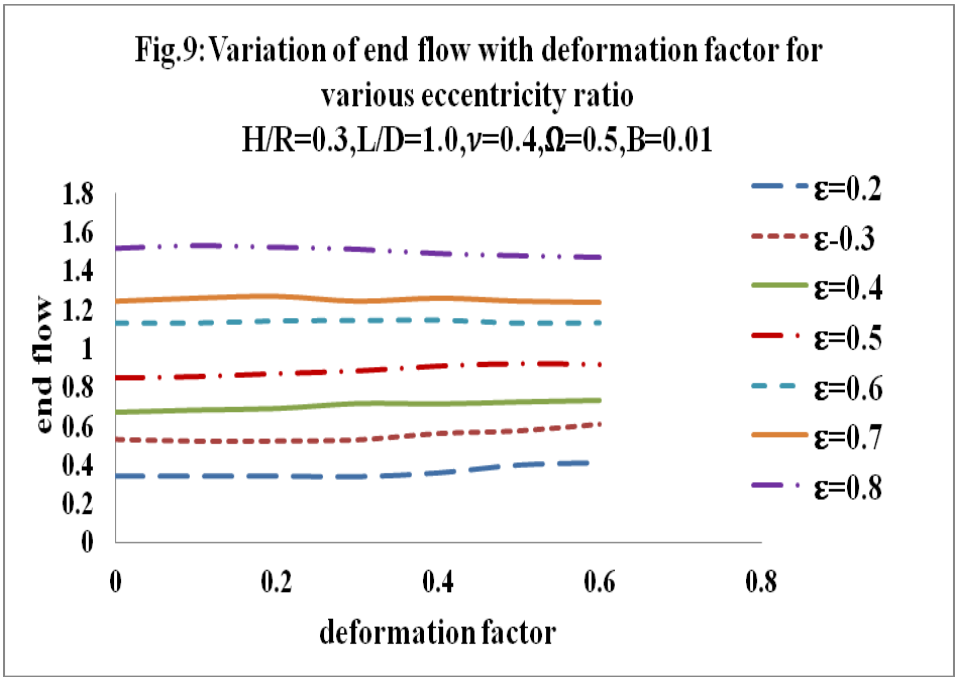

Figure.10 shows the comparison of dimensionless load carrying capacity with respect to deformation factor for working fluid with constant & variable viscosity when other parameters taken as $\frac{L}{D}=1.0,\ \frac{H}{R}=0.3,\ \nu=0.4, \varepsilon_0=0.6$.

It can be seen that load carrying capacity increase with increase viscosity parameter B.

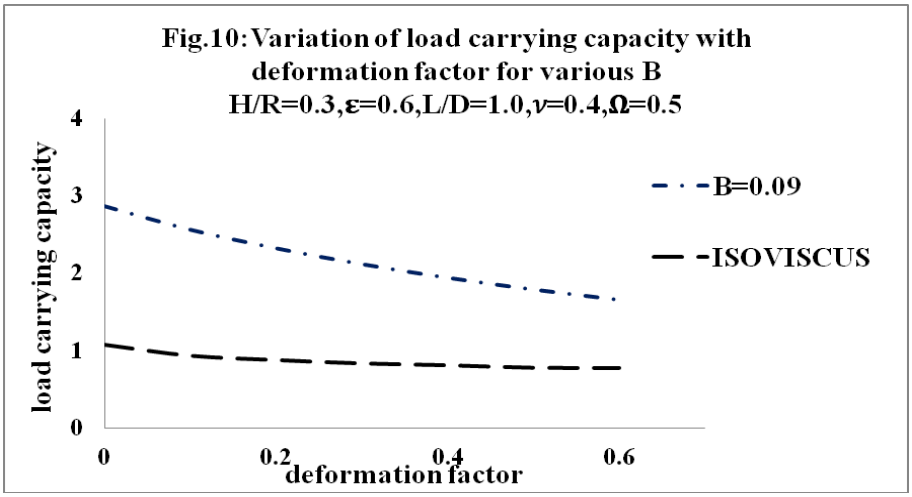

VI. CONCLUSIONS

Numerical methods are used to determine the effects of elastic distortions in the bearing liner on bearing performance of finite journal bearing:

1. The region of load carrying capacity decreases as the bearing liner is made more flexible for high eccentricity ratios (i.e., ε_0 > 0.8). For ε_0 < 0.6, the flexibility of the bearing liner had little or no effect on stability.
2. As L/D is increased, distortion effects are more prominent. This leads to a decrease in load carrying capacity.
3. The hydrodynamic pressure and hence the load capacity is reduced as the bearing liner becomes more flexible, especially at eccentricities greater than 0.8.
4. As the viscosity parameter B increases the load carrying capacity increases but drop when bearing liner is made more flexible
5. As the Poisson ratio increases the load carrying capacity increases but drop sharply when bearing liner is made more flexible.
6. As the liner thickness to radius ratio increases the load carrying capacity decreases but drop when bearing liner is made more flexible

NOMENCLATURE:

$a = r_i$	Inner radius of the bearing liner [m]
$b = r_0$	Outer radius of the bearing liner [m]
c	Radial clearance [m]
R	Journal radius [m]
D	Journal diameter [m]
$d_{m,n}$	Distortion coefficient of $_{m,n}$ harmonic
m,n	Axial and circumferential harmonics
e	Eccentricity [m]
e_0	Steady state eccentricity [m]
E	Young's modulus [N / m^2]
F	Elasticity parameter or deformation factor, $= \frac{\eta_0 R^3 \omega}{c^3 E}$
F_S	Shear force on journal surface [N]
$\bar{F}_r$	Nondimensional fluid film force along the line of centers
$\bar{F}_\phi$	Nondimensional fluid film force perpendicular the line of centres

$\bar{F}_{r_0}$, $\bar{F}_{\phi_0}$	Non-dimensional steady state fluid film forces
h	Oil film thickness [m]
h_0	Steady state oil film thickness [m]
$\bar{h}$	Non-dimensional oil film thickness
H	Thickness of bearing liner [m]
L	Length of bearing [m]
p	Oil film pressure [Pa]
p_0	Steady state film pressure [Pa]
$\bar{p}$	Dimensionless oil pressure
Q	End flow of oil [m^3/s]
$\bar{Q}$	Nondimensional End flow
$\bar{u}, \bar{v}, \bar{w}$	Components of fluid velocity in the x, y, and z direction, respectively. [m/s]
U	Shaft peripheral speed [m/s]
W_0	Steady state load [N]
$\bar{W}_0$	Dimensionless steady state load
x, y, z	Circumferential, radial and axial coordinates
$\theta, \bar{y}, \bar{z}$	Dimensionless coordinates in circumferential, radial and axial directions
η_0	Viscosity at inlet condition [Pa s]
$\bar{\eta}$	Non-dimensional viscosity of oil
ρ	Density [kg/m^3]
ν	Poisson's ratio
ε	Eccentricity ratio
ε_0	Steady state eccentricity ratio
ϕ	Attitude angle [rad]
ϕ_0	Steady state attitude angle [rad]
θ_1	Angular coordinates at which the fluid film commences [rad]
θ_2	Angular coordinates at which the fluid film cavitates [rad]
δ	Deformation of bearing surface. [m]
δ_0	Steady state deformation of bearing surface. [m]
$\bar{\delta} = \delta/c$	Non-dimensional deformation of bearing surface
λ, μ	Lame's constants
$B = \frac{\eta_0 \alpha \omega R^2}{c^2}$	Viscosity Parameter

REFERENCES

[1] N.P.Petroff, "Friction in machines and the effect of lubricant," Engg. Journal, St. Petersburg, No. 1,2,3,4, 1983.

[2] B.Tower, "1st report on friction experiments, "Proc. Inst. Mech. Engrs., 1883, 632-664, 1884, 29-35; Part II: 1885, 58-70; Part III: 1888, 173-205; Part IV:1891, 111-140.

[3] O.Reynolds, "On the theory of lubrication and its application to Mr. Beauchamp Tower's experiments, including an experimental determination of the viscosity of Olive oil," Phil. Trans. Royal Soc., London, 177, 1886, 157-234.

[4] H.N.Chandrawat and R Sinhasan, "A study of steady state and transient performance characteristics of a flexible shell Journal bearing," Tribology International, V21, n3, Jun 1988, pp 137 - 148.

[5] R. Pai and B.C.Majumder, "Stability of submerged oil Journal bearing under dynamic load," Wear V146, n1, May 30, 1991, pp 125 - 135.

[6] B.C.Majumder and M.K.Ghosh, "Stability of a rigid rotor supported on rough oil journal bearings," Trans. ASME, J.Tribology, 112, 1990, pp 73-77.

[7] H.D.Conway and H.C.Lee, "The analysis of the lubrication of a flexible Journal bearing,"ASME Journal of Lubrication Technology, Vol 97, n4, 1975, pp 599–604.

[8] B.C.Majumder, D.E.Brewe and M.M.Khonsari, "Stability of a rigid rotor supported on flexible oil Journal bearings," Journal of Tribology Trans Vol 110, 1988, pp 181 - 187.

[9] J.O'Donoghue, D.K.Brighton and C.J.K.Hooke, "The effect of elastic distortions on Journal bearing performance," Journal of Lubrication Technology, Vol 89, n4, 1967, pp 409 -417.

[10] D.K.Brighton, C.J.K.Hooke and J.O'Donoghue , "A theoretical and experimental investigation on the effect of elastic distortions on the performance of Journal bearing," Tribology convention 1968, Proc. of Institute of Mechanical Engineers, Vol 182,Part 3N, 1967 - 1968, pp 192 - 200.

[11] B.C.Majumder and D.E.Brewe, "Stability of a rigid rotor supported on oil film journal bearings under dynamic load," NASA TM, 102309, 1987.

[12] S.C.Jain, R.Sinhasan and D.V.Singh, "Elastohydrodynamic analysis of a cylindrical Journal bearing with a flexible bearing shell," Wear, March 1981, pp 325 - 335.

[13] H.D.Conway, H.C.Lee., "The Analysis of the Lubrication of a flexible Journal Bearing" Transaction of ASME, Journal of Lubrication Technology, October 1975, pp 599-604

[14] Jose´ A. Va´zquez, Lloyd E. Barrett, Ronald D. Flack "A Flexible Rotor on Flexible Bearing Supports: Stability and Unbalance Response" Transactions of the ASME, Journal of Vibration and Acoustics, APRIL 2001, Vol. 123 pp 137-144

[15] Benasciutti, M. Gallina, M. Gh. Munteanu, F. Flumian,2012 "A Numerical Approach for Static and Dynamic Analysis of Deformable Journal Bearings" World Academy of Science, Engineering and Technology 67 , 2012,pp-778-783

[16] D.G.Christopherson, "A new mathematical model for solution of film lubrication problems," Proc. Inst. Mech. Engrs., London, 146, 1942, 126-135.

[17] A.A.Raimondi and J.Boyd, "A solution for the finite journal bearing and its application to analysis and design," I, II, III, ASLE Trans., 1958, 159-209.

[18] Oh, K. P., and Huebner, K. H., "Solution of the Elastohydrodynamic Finite Journal Bearing Problem," ASME JOURNAL OF LUBRICATION TECHNOLOGY, Vol. 95, No. 3, 1973, pp. 342-352.

[19] H.G.Elrod, "A cavitation algorithm," Trans. ASME, J. Lub. Tech., 103, 1981, 350-354.

[20] Capone, "Oil whirl in Journal bearing under no load conditions," Wear V26, n2, Nov 1973 pp 207 - 217.

[21] Cameron, "Basic Lubrication theory," Longman Group Ltd., 1970

[22] M. K. Ghosh, B.C.Majumder & Mihir Sarangi, "Theory of Lubrication", Tata McGraw Hill company.

[23] B.C.Majumder, "Introduction to Tribology of Bearings," A.H.Wheeler & Co., 1986.

[24] Bernard J. Hamrock, "Fundamentals of Fluid flim Lubrication," McGraw Hill International edition, 1994

[25] S.P.Timoshenko and J.N.Goodier, "Theory of Elasticity," McGraw Hill Book Company, 1987